American Industrial Hygiene Association Journal

ISSN: 0002-8894 (Print) (Online) Journal homepage: https://www.tandfonline.com/loi/aiha20

Prediction and Measurement of Velocity into Flanged Slot Hoods

LORRAINE M. CONROY , MICHAEL J. ELLENBECKER & MICHAEL R. FLYNN

To cite this article: LORRAINE M. CONROY , MICHAEL J. ELLENBECKER & MICHAEL R. FLYNN (1988) Prediction and Measurement of Velocity into Flanged Slot Hoods, American Industrial Hygiene Association Journal, 49:5, 226-234, DOI: 10.1080/15298668891379657

To link to this article: https://doi.org/10.1080/15298668891379657

Am. Ind. Hyg. Assoc. J. 49(5):226-234 (1988)

Prediction and Measurement of Velocity into Flanged Slot Hoods

LORRAINE M. CONROY[A], MICHAEL J. ELLENBECKER[B] and MICHAEL R. FLYNN[C]

[A]Harvard University, School of Public Health, Department of Environmental Sciences and Physiology, 665 Huntington Ave., Boston, MA 02115; [B]University of Lowell, Work Environment Department, One University Ave., Lowell, MA 01854; [C]University of North Carolina, School of Public Health, Department of Environmental Sciences and Engineering, Chapel Hill, NC 27514

A model describing the three-dimensional velocity field into a flanged slot hood has been developed using potential flow theory. Modeling the slot as an elliptical aperture allows use of the potential function to develop expressions for the velocity components (v_x,v_y,v_z) at any point (x,y,z). Experiments were performed to measure velocities in front of six slot hoods. Experimental results were compared with velocities predicted by two models: an equal area ellipse with the same length to width ratio as the slot and an ellipse inscribed within the slot.

Introduction

A slot hood is one example of an exterior hood. Slot hoods commonly are used to provide uniform exhaust airflow over a finite length of contaminant generation such as an open surface tank or a workbench.

The American Conference of Governmental Industrial Hygienists (ACGIH) industrial ventilation manual[1] describes the current design method for exterior hoods. First, disturbing air movements in the vicinity of the hood are eliminated or minimized; second, the hood is located as close as practicable to the source; and third, the capture velocity is determined. The manual defines capture velocity as "the air velocity at any point in front of the hood or at the hood opening necessary to overcome opposing air currents and to capture the contaminated air at that point by causing it to flow into the hood."[1] The selected value of capture velocity depends on the release velocity of the contaminant and the magnitude of disturbing room air currents.

DallaValle,[2] Silverman,[3-6] Garrison,[7-9] Fletcher,[10,11] and Fletcher and Johnson[12] have presented empirical expressions for centerline velocity as a function of hood shape, airflow into the hood (Q), centerline distance of the source from the hood (X), and hood area (A). The airflow necessary to obtain the desired capture velocity is calculated using one of these empirical expressions. Additional empirical factors sometimes are introduced to account for high toxicity of the contaminant and disruptive air movements caused by hot processes.

For sources which cover considerable area or are in locations subject to drafts, centerline velocity prediction will not give sufficient information for an accurate prediction of hood performance. Since slot hoods usually are used to exhaust area sources, the current design method for these devices may give unsatisfactory results. What is needed is a design procedure which quantitatively accounts for crossdrafts and area sources.

This paper represents the first step in the development of a quantitative technique for the design of slot hoods used for area sources located in any type of crossdraft. Potential flow theory has been used to develop expressions for the velocity components (v_x,v_y,v_z) at any point (x,y,z) in front of a flanged slot hood.

Theory

The continuity equation for frictionless incompressible flow is

$$\nabla \cdot V = 0 \qquad (1)$$

where V is the velocity. If the flow also is irrotational,

$$V = \nabla \phi \qquad (2)$$

or

$$V_x = \frac{\partial \phi}{\partial x} \qquad V_y = \frac{\partial \phi}{\partial y} \qquad V_z = \frac{\partial \phi}{\partial z} \qquad (3)$$

where ϕ is the scalar velocity-potential function, and the continuity equation becomes Laplace's equation

$$\nabla^2 \phi = 0 \qquad (4)$$

Analysis of Laplace's equation is developed well and is termed potential theory.[13]

Rectangular openings are difficult to model using potential flow theory because an analytic solution for the potential

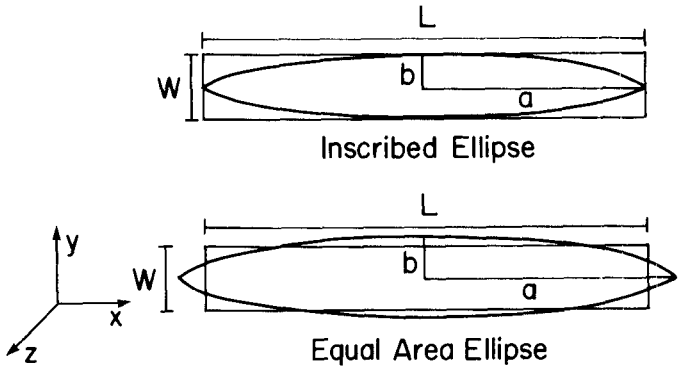

Figure 1—Inscribed and equal area ellipses as models of length (L) and width (W) for a slot.

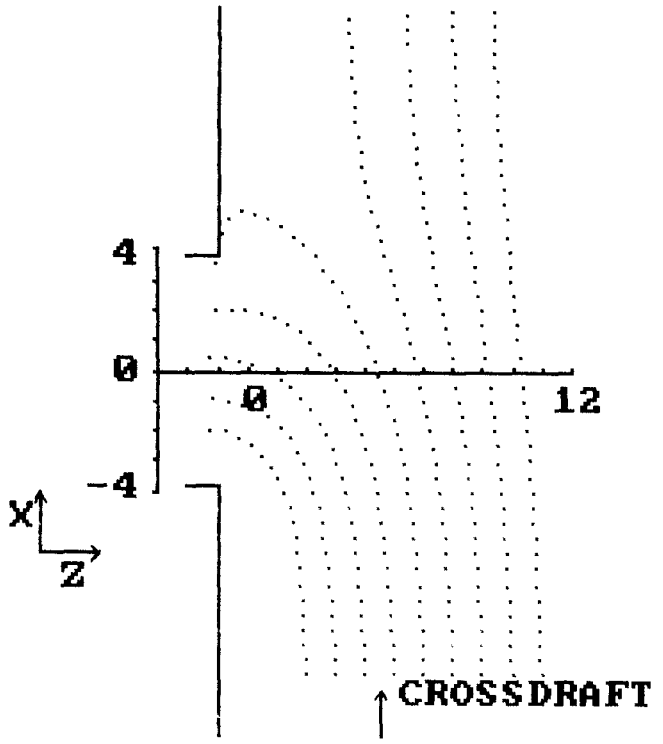

Figure 2—Airflow streamlines for a 0.19 m × 0.0381 m (7.5 in. × 1.5 in.) hood with a face velocity of 5.1 m/s (1000 fpm) and a crossdraft velocity of 0.51 m/s (100 fpm) using model 1 [slot viewed from top (y = 0, xz-plane)].

is not available. The solution for an elliptical aperture was determined by Lamb,[14] who suggests two different models of a rectangular slot: 1) an inscribed ellipse where the major axis (2a) equals the slot length and the minor axis (2b) equals the slot width; and 2) an ellipse with the same area and aspect ratio as the slot, that is, $\pi ab = LW$ and $a/b = L/W$. Figure 1 illustrates these two models.

The potential function for flow through an elliptical aperture with a constant potential across the hood face is[14]

$$\phi = \mp \frac{Q}{4\pi} \int_0^{\lambda} \frac{d\lambda}{[(a^2 + \lambda)(b^2 + \lambda)\lambda]^{1/2}} \quad (5)$$

where λ is the positive root of

$$\frac{x^2}{a^2 + \lambda} + \frac{y^2}{b^2 + \lambda} + \frac{z^2}{\lambda} = 1 \quad (6)$$

The potential equation can be solved to give the velocity components in the x, y and z directions, where x is parallel to the hood length, y is parallel to the hood width, and z is perpendicular to the hood face (Figure 1). The velocity at any point can be determined using the following expressions:[15]

$$V_x = \frac{dx}{dt} = \frac{\partial \phi}{\partial x} = \frac{Qx(a^2 + \lambda)^{1/2}(b^2 + \lambda)^{3/2}\lambda^{3/2}}{2\pi E} \quad (7)$$

$$V_y = \frac{dy}{dt} = \frac{\partial \phi}{\partial y} = \frac{Qy(a^2 + \lambda)^{3/2}(b^2 + \lambda)^{1/2}\lambda^{3/2}}{2\pi E} \quad (8)$$

$$V_z = \frac{dz}{dt} = \frac{\partial \phi}{\partial z} = \frac{Qz(a^2 + \lambda)^{3/2}(b^2 + \lambda)^{3/2}\lambda^{1/2}}{2\pi E} \quad (9)$$

where

$$E = x^2\lambda^2(b^2 + \lambda)^2 + y^2\lambda^2(a^2 + \lambda)^2 + z^2(a^2 + \lambda)^2(b^2 + \lambda)^2 \quad (10)$$

The use of this potential flow solution in describing actual velocity fields may be somewhat limited because it assumes a constant potential across the hood face. This boundary condition leads to predicted velocities of one-half the average face velocity at the center of the hood face and infinite velocities at the edges of the ellipse. This suggests that modification to improve the exact solution may be possible.

For the case of circular hoods, Flynn and Ellenbecker[16] observed that the velocity contours obtained by DallaValle[2] have a distinctly elliptic shape suggesting that equal velocity surfaces may be coincident with equipotential surfaces. In general this is not true in potential flow theory, where the velocity is the gradient of the potential.

Assuming that surfaces of constant velocity coincide with equipotential surfaces, an approximation of the magnitude of the velocity can be determined at any point using the following equation:[15]

$$\frac{ds}{dt} = \frac{\sqrt{3}Q}{2\pi[3\lambda^2 + 2(a^2 + b^2)\lambda + a^2b^2]^{1/2}} \quad (11)$$

The direction of the velocity can be determined from the exact solution. Flynn and Ellenbecker[17] suggested that this solution somehow corrected for the neglect of frictional forces and the boundary conditions of constant potential at the hood face. Details of these derivations are given in the appendix.

Computer programs have been written which use the exact potential flow solution (Equations 7–9) and the approximate solution (Equation 11) to generate streamlines of velocity in front of a hood for both an inscribed ellipse and an equal area ellipse. Crossdrafts can be added to each model by simple vector addition of the velocity components. An example of the output from these programs, showing a slot hood in a uniform crossdraft of 0.51 m/s (100 fpm) in the x-direction, is given in Figure 2.

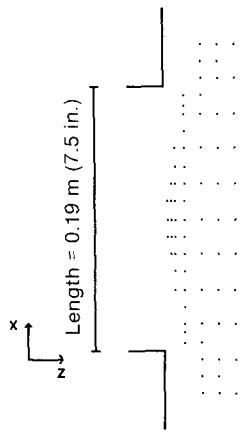

Figure 3—Sampling points in front of the 0.19 m (7.5 in.) long hoods.

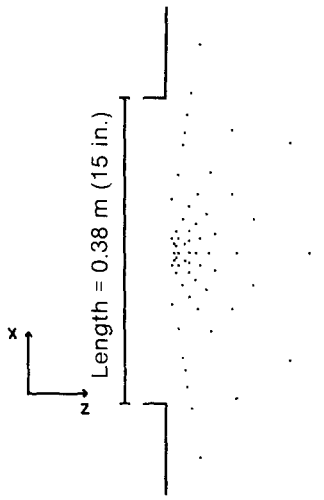

Figure 4—Sampling points in front of the 0.38 m (15 in.) long hoods.

Experimental Procedure

A series of experiments was performed to test the theoretical models. Flanged slot hoods of 2 lengths [0.19 and 0.38 m (7.5 and 15 in.)] and 3 aspect ratios (15:1, 10:1 and 5:1) were studied. Each hood was operated at average face velocities of 5.1, 10.2 and 15.2 m/s (1000, 2000 and 3000 fpm). These measurements were conducted in an unventilated chamber so that extraneous crossdrafts were minimized and the models could be tested in a valid manner. Points were chosen in front of each hood (Figures 3 and 4) to cover the entire field, such that the points furthest from the hood corresponded to velocities equal to approximately 5% of the face velocity.

The 0.19 m (7.5 in.) hoods were studied initially, and points were chosen in a rectangular pattern to cover the entire field. Points close to the flange were not chosen because the model was expected to predict very poorly in this area. This area is not important in future capture efficiency models because a source of contaminant would not be located in an area very close to the flange. When looking at the 0.38 m (15 in.) hoods, the pattern of measurement points was changed in order to cover the area of velocity contours of 100% to 5% of the face velocity with approximately the same number of measurement points as with the 0.19 m (7.5 in.) hoods.

Velocities were measured using a TSI Corporation hot-film anemometer with a two-wire, mutually-perpendicular probe (model numbers 1501-2, 1054-B and 1240-20, TSI Corporation, St. Paul, Minn.) designed for crossflow applications. The anemometer measures velocity in two dimensions and was used in the horizontal centerline plane (the xz-plane). It was attached to a lathe bed which allowed accurate and reproducible positioning. Figure 5 shows the experimental apparatus.

Results

Experimentally measured x and z velocity components were compared with values predicted by four theoretical models:

1) inscribed ellipse, exact solution;
2) inscribed ellipse, approximate solution;
3) equal area ellipse, exact solution; and
4) equal area ellipse, approximate solution.

A least squares performance index (I) and a bias index (Δ) were calculated for each theoretical model. The performance index is defined as the mean of the squares of residuals,

$$I = \Sigma(P - M)^2/N \quad (12)$$

and the bias index (Δ) is defined as the mean of the residuals,

$$\Delta = \Sigma(P - M)/N \quad (13)$$

where P = predicted velocity, M = measured velocity and N = number of measurements.[18,19] Table I displays the value of I and Δ for each model for both the x- and z-components of velocity. The best model is one in which I is a minimum and Δ is closest to zero.

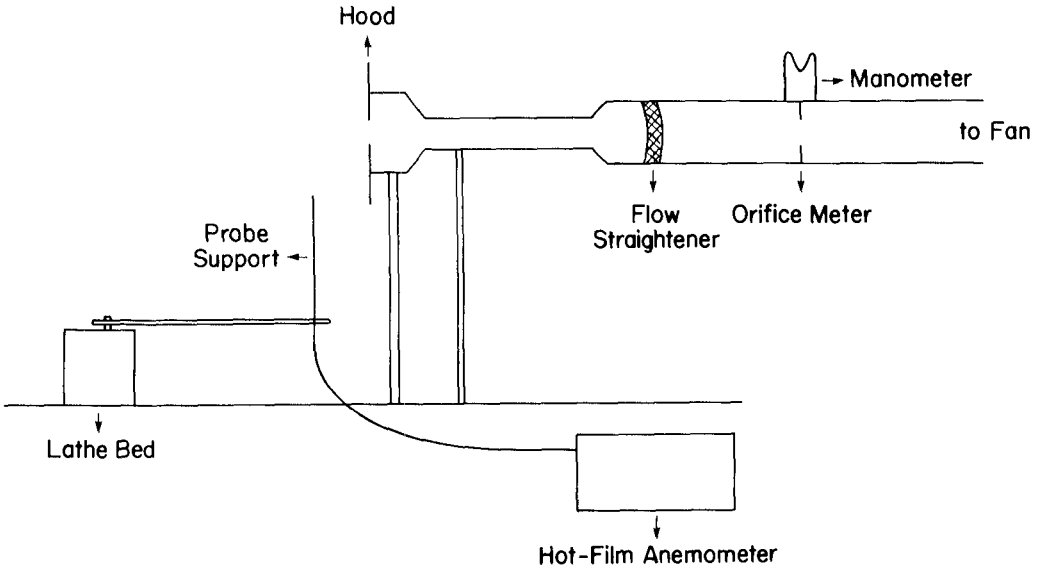

Figure 5—Experimental apparatus.

TABLE I
Performance Index, Bias Index and Analysis of Variance Results for Each Velocity Model

	X-Component of Velocity			
	Model			
	1	2	3	4
Δ	-0.1	-3.8	-9.6	-11.6
I	754.7	1601.8	3753.5	4348.7
Length	ns[A]	ns	ns	ns
Aspect ratio	s[B]	s	s	s
Face velocity	s	s	s	s
X	ns	s	s	s
Z	ns	ns	ns	ns

	Z-Component of Velocity				
	Model				
	1	2	3	4	1 corrected
Δ	-66.9	102.7	-146.1	9.5	22.2
I	29 848.9	34 309.5	82 503.6	6061.9	4976.7
Length	s	s	ns	s	s
Aspect ratio	s	s	s	s	s
Face velocity	s	s	s	s	s
X	s	ns	s	s	ns
Z	s	s	s	s	s

[A]ns = not significant.
[B]s = significant, $p < 0.01$.

Model 1 is the best predictor of velocity in the x-direction with both I and Δ much less than with the other three models. Model 4 is the best predictor of the z-component of velocity with Model 1 being the next best. Model 4, however, is the worst predictor of x-component velocity (has the largest value of performance index and the greatest bias). For this reason Model 1, the inscribed ellipse, exact solution model, was chosen as the best predictor of velocity.

An attempt was made to empirically correct the Model 1 z-component. The agreement between predicted and measured velocity changes as a function of location in front of the hood. The agreement is better further from the hood face than close to it, for reasons explained below. A factor was determined which forces the slope of the measured versus predicted line to equal one. This factor is a function of λ, which in turn is a function of x, y and z locations in front of the hood. The predicted z-component velocity (Equation 9) is multiplied by this factor,

$$\frac{\ln \lambda - 11.8}{-10.7}$$

to give a corrected z-velocity. The performance index, bias index and analysis of variance results also are given in Table 1 in the column labeled Model 1 corrected.

Analysis of variance for the factors length, aspect ratio, face velocity and x- and z-locations in front of the hood shows aspect ratio and face velocity to contribute significantly to explaining the observed variance with Model 1 for the x-velocity. For the z-component of velocity, all of the factors except x-location contribute significantly to explaining the observed variance. Comparisons of measured versus predicted velocities using Model 1 to predict the x-component and using the empirically corrected Model 1 to predict the z-component are displayed in Figures 6 and 7.

Discussion

The equal area ellipse model overlaps the flange on the two centerlines and, thus, predicts flow where there is none. The inscribed ellipse model assumes a flange in the corners where the rectangular experimental hood does not have one and, therefore, predicts no flow where there is flow. In actual practice little flow may occur in the corners because of turbulence caused by the sharp edges and *vena contracta* formation. This may explain why the inscribed ellipse (Models 1 and 2) is a better predictor of performance. By using an inscribed ellipse, the model assumes there is no flow in the corners and potential flow across the region enclosed by the inscribed ellipse.

The anemometer measures velocity in two dimensions. Because of this constraint, velocity was measured in the horizontal centerline plane only. In this plane the inscribed ellipse is the same length as the experimental hoods. No measurements were made in the area where the inscribed ellipse model was most likely to fail, *i.e.*, the corners. Measurements also were not made in the area where the equal area ellipse was most likely to fail: along the centerline very close to the flange. Nevertheless, the choice of measurement points may have biased the results toward the inscribed ellipse model.

Both theories inadequately predict performance on or very near the hood face. The exact solution predicts velocity to be one-half of the face velocity at the center of the hood face and to be infinite at the edges. Experimental velocities near the center of the hood face lie above the 45° line, indicating that theory underpredicts experimental velocity in this area. Velocities near the edges of the hood face lie below the 45° line, indicating that theory overpredicts experimental velocity here.

The approximate solution predicts a more uniform velocity across the face of the hood but with a lower average value, *i.e.*, approximately 87% of the average face velocity. The approximate solution assumes that equipotential surfaces and equal velocity contours are coincident. This is not predicted by potential flow theory, which could explain why the approximate solution underpredicts velocity.

In any case, Model 1 with the z-component empirically corrected is an excellent predictor of both components of velocity.

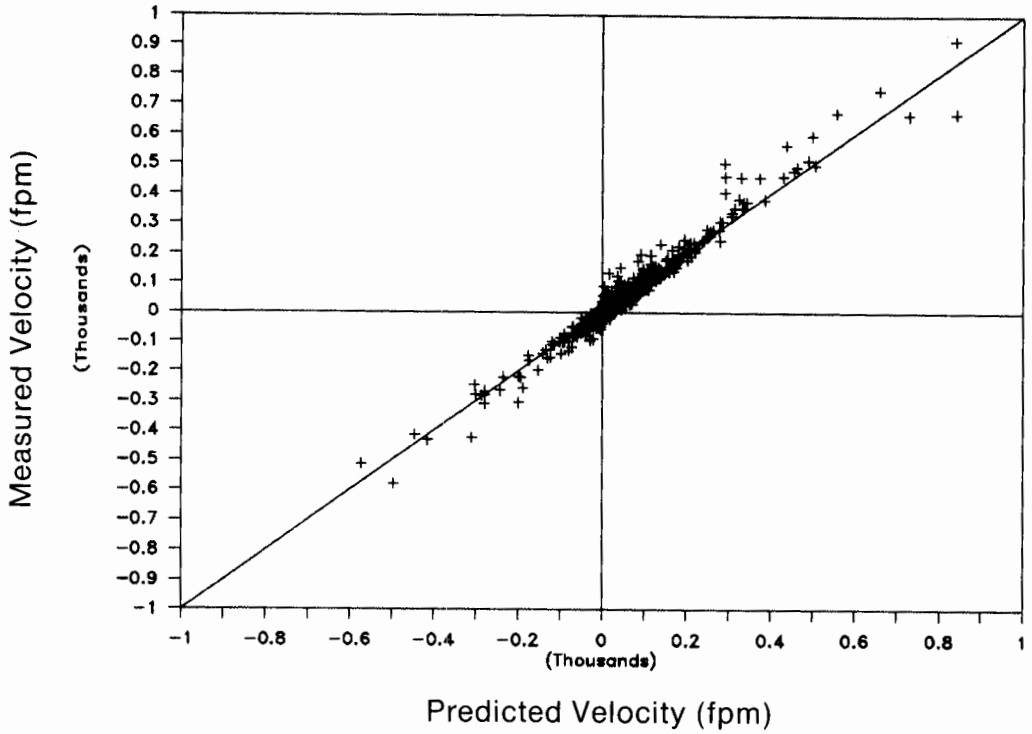

Figure 6—Experimental versus theoretical velocities in the x-direction—theoretical velocities were calculated using model 1.

Comparison with Previous Investigations

Flynn and Ellenbecker[17] used circular hoods, so their theoretical and experimental hoods were identical. They found the approximate solution—equipotential surfaces coincident with equal velocity surfaces—to be the best predictor of velocity. They suggested that this solution corrected for frictional forces near the hood face and the assumed constant potential at the hood face. This solution was used to predict the axial, or z-component, of velocity; and the radial, or x-component, of velocity was corrected empirically to

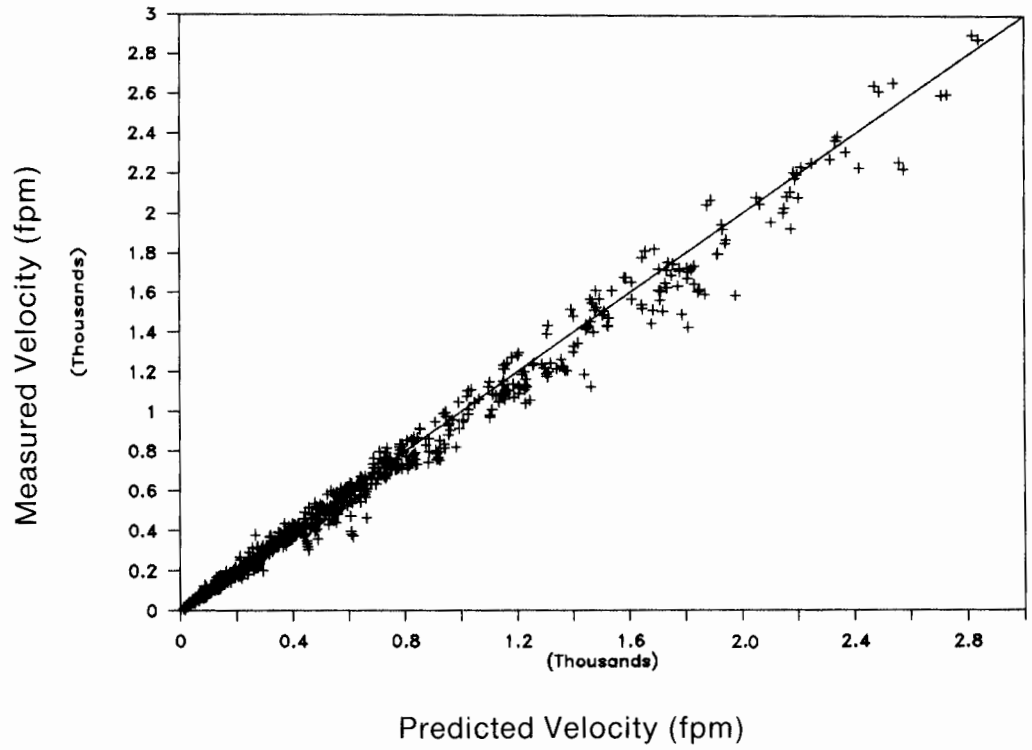

Figure 7—Experimental versus theoretical velocities in the z-direction—theoretical velocities were calculated using the empirically corrected model 1.

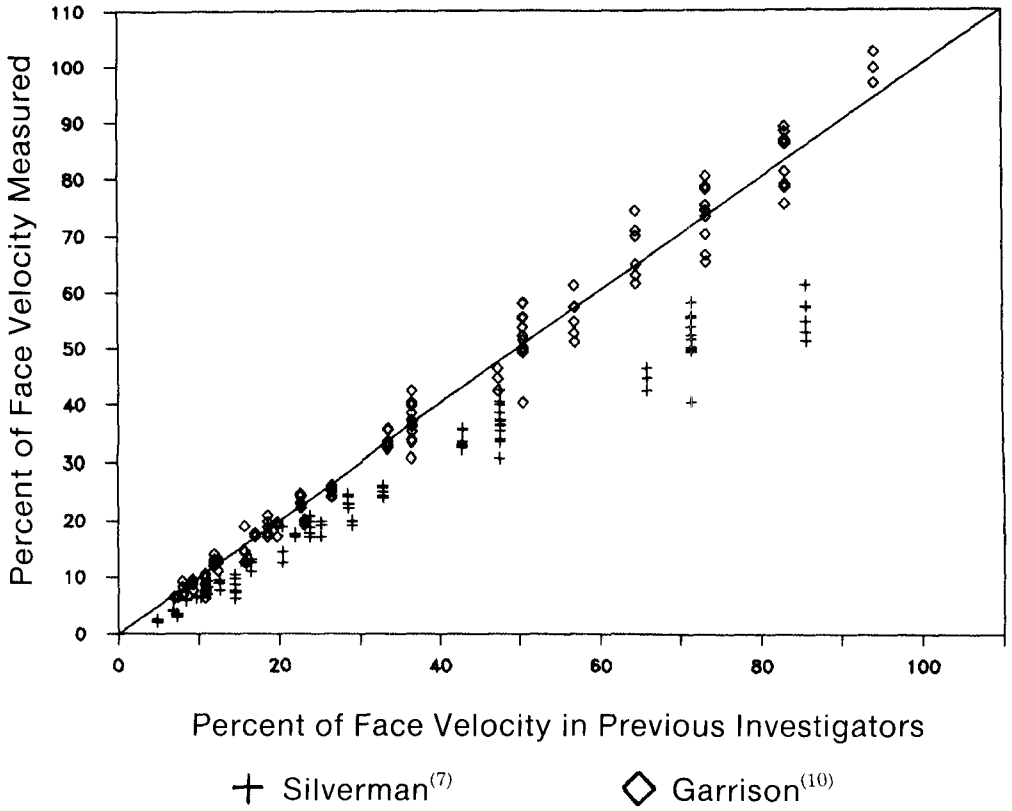

Figure 8—Centerline velocity, experimental velocities compared with those of previous investigations.

give better agreement between theory and experiment. Their results agree with the results of the present experiments to the extent that when using an equal area ellipse model, the approximate solution predicts the z-component better than the exact solution. The x-component is not predicted well using either the exact or approximate solution for an equal area ellipse.

Experimental centerline values measured here are compared with those of Silverman[6] and Garrison[9] in Figure 8. Silverman's equation is limited to values away from the hood ($z/W > 0.4$). Garrison developed a model for centerline velocity for high velocity/low volume exhaust systems. The experimental data agree well with these models, especially at the lower velocities.

Conclusions

Several important conclusions can be reached based on this work.

1) The inscribed ellipse model with the exact solution is the best predictor of experimental velocity.

2) The velocity at any point in a flow field can be predicted using this model, which represents a significant improvement over current design equations which predict only the centerline velocity.

3) Centerline experimental data agree well with results of previous investigators.

4) The potential flow solution presented here is the general case for elliptical openings. The solution for circular hoods (where the aspect ratio equals one), presented previously by Flynn and Ellenbecker,[16] is one example of this more general solution.

5) Crossdrafts and other disruptive air movements can be added to this model through the use of simple vector addition, as shown in Figure 2.

6) Capture efficiency is a more direct index of hood performance than capture velocity[20] and, therefore, is a more useful concept in ventilation design and for estimating worker exposure to toxic contaminants. For this reason the velocity model presented here, with the addition of crossdrafts, is being used to develop a model for capture efficiency of flanged slot hoods.

Acknowledgments

This work was supported by the American Society of Heating, Refrigerating and Air-Conditioning Engineers (ASHRAE) Grant-in-Aid program and the Occupational Safety and Health Educational Resource Center National Institute for Occupational Safety and Health (NIOSH) grant award 5 T15 OH07096 at the Harvard School of Public Health.

References

1. **American Conference of Governmental Industrial Hygienists:** *Industrial Ventilation—A Manual of Recommended Practice,* by the Committee on Industrial Ventilation. 17th ed. Lansing, Mich.: American Conference of Governmental Industrial Hygienists, 1982. pp. 4-1-4-21.
2. **DallaValle, J.M.:** "Studies in the Design of Local Exhaust Hoods." Sc.D. diss. Harvard University, 1930.

3. **Silverman, L.:** Fundamental Factors in the Design of Lateral Exhaust Hoods for Industrial Tanks. *J. Ind. Hyg. Toxicol. 23(5)*:187-266 (1941).
4. **Silverman, L.:** Centerline Velocity Characteristics of Round Openings under Suction. *J. Ind. Hyg. Toxicol. 24(9)*:259-266 (1942).
5. **Silverman, L.:** Velocity Characteristics of Narrow Exhaust Slots. *J. Ind. Hyg. Toxicol. 24(9)*:267-276 (1942).
6. **Silverman, L.:** "Fundamental Factors in the Design of Exhaust Hoods." Sc.D. diss., Harvard University, 1943.
7. **Garrison, R.P.:** "Nozzle Performance and Design for High Velocity/Low Volume Exhaust Ventilation." Ph.D. diss., University of Michigan, 1977.
8. **Garrison, R.P.:** Centerline Velocity Gradients for Plain and Flanged Local Exhaust Inlets. *Am. Ind. Hyg. Assoc. J. 42*:739-746 (1981).
9. **Garrison, R.P.:** Velocity Calculation for Local Exhaust Inlets—Empirical Design Equations. *Am. Ind. Hyg. Assoc. J. 44*:937-940 (1983).
10. **Fletcher, B.:** Centerline Velocity Characteristics of Rectangular Unflanged Hoods and Slots under Suction. *Ann. Occup. Hyg. 20*:141-146 (1977).
11. **Fletcher, B.:** Effect of Flanges on the Velocity in front of Exhaust Ventilation Hoods. *Ann. Occup. Hyg. 21*:265-269 (1978).
12. **Fletcher, B. and A.E. Johnson:** Velocity Profiles around Hoods and Slots and the Effects of the Adjacent Plane. *Ann. Occup. Hyg. 25*:365-372 (1982).
13. **White, F.:** *Fluid Mechanics.* New York: McGraw-Hill, 1982. pp. 454-456.
14. **Lamb, H.:** *Hydrodynamics.* 6th ed. New York: Dover Publications, 1945. pp. 148-152.
15. **Flynn, M.R.:** "The Capture Efficiency of Local Exhaust Hoods." Sc.D. diss., Harvard University, 1986.
16. **Flynn, M.R. and M.J. Ellenbecker:** The Potential Flow Solution for Air Flow into a Flanged Circular Hood. *Am. Ind. Hyg. Assoc. J. 46*:318-322 (1985).
17. **Flynn, M.R. and M.J. Ellenbecker:** Empirical Validation of Theoretical Velocity Fields into Flanged Circular Hoods. *Am. Ind. Hyg. Assoc. J. 48*:380-389 (1987).
18. **Rudnick, S.N., J.L.M. Koehler, K.P. Martin, D. Leith and D.W. Cooper:** Particle Collection Efficiency in a Venturi Scrubber: Comparison of Experiments with Theory. *Environ. Sci. Technol. 20(3)*:237-242 (1986).
19. **Koehler, J.L.M.:** "Effects of Liquid Utilization on Venturi Scrubber Performance." Sc.D. diss., Harvard University, 1986.
20. **Flynn, M.R. and M.J. Ellenbecker:** Capture Efficiency of Flanged Circular Exhaust Hoods. *Ann. Occup. Hyg. 30(4)*:497-513 (1986).

APPENDIX

Lamb[1] gives the potential function for flow through an elliptic aperture in a thin plane wall as the following:

$$\phi = \mp \frac{Q}{4\pi} \int_0^{\lambda} \frac{d\lambda}{[(a^2 + \lambda)(b^2 + \lambda)\lambda]^{1/2}} \quad \text{(A1)}$$

where the upper limit is the positive root of

$$\frac{x^2}{a^2 + \lambda} + \frac{y^2}{b^2 + \lambda} + \frac{z^2}{\lambda} = 1 \quad \text{(A2)}$$

The elliptic aperture is situated in the xy-plane and is the region enclosed by the ellipse:

$$\frac{x^2}{a^2} + \frac{y^2}{b^2} = 1 \quad \text{(A3)}$$

and the z axis is the hood centerline. The volume flow into the hood is Q.

The potential function (Equation A1) is an elliptic integral, and an analytic solution is not possible. The velocity components (v_x,v_y,v_z) at any point (x,y,z), however, can be obtained.

Lamb[14] presents the solution to Equation A2 in the elliptical coordinate system developed by Lamé (λ,μ,υ) related to cartesian coordinates by the following:

$$x^2 = \frac{(a^2 + \lambda)(a^2 + \mu)(a^2 + \upsilon)}{(a^2 - b^2)(a^2 - c^2)} \quad \text{(A4)}$$

$$y^2 = \frac{(b^2 + \lambda)(b^2 + \mu)(b^2 + \upsilon)}{(b^2 - a^2)(b^2 - c^2)} \quad \text{(A5)}$$

$$z^2 = \frac{(c^2 + \lambda)(c^2 + \mu)(c^2 + \upsilon)}{(c^2 - a^2)(c^2 - b^2)} \quad \text{(A6)}$$

The surfaces λ,μ,υ are ellipsoids, hyperboloids of one sheet, and hyperboloids of two sheets, respectively.

Equations A4–A6 give

$$\frac{\partial x}{\partial \lambda} = \frac{1}{2} \frac{x}{a^2 + \lambda} \quad \text{(A7)}$$

$$\frac{\partial y}{\partial \lambda} = \frac{1}{2} \frac{y}{b^2 + \lambda} \quad \text{(A8)}$$

$$\frac{\partial z}{\partial \lambda} = \frac{1}{2} \frac{z}{c^2 + \lambda} = \frac{1}{2} \frac{z}{\lambda} \quad \text{(A9)}$$

for z = centerline axis, c = 0.

If x,y,z are functions of the three parameters λ,μ,υ such that the surfaces λ = constant, μ = constant and υ = constant are mutually orthogonal at their intersections, and if

$$\frac{1}{h_1^2} = \left[\frac{\partial x}{\partial \lambda}\right]^2 + \left[\frac{\partial y}{\partial \lambda}\right]^2 + \left[\frac{\partial z}{\partial \lambda}\right]^2 \quad \text{(A10)}$$

$$\frac{1}{h_2^2} = \left[\frac{\partial x}{\partial \mu}\right]^2 + \left[\frac{\partial y}{\partial \mu}\right]^2 + \left[\frac{\partial z}{\partial \mu}\right]^2 \quad \text{(A11)}$$

$$\frac{1}{h_3^2} = \left[\frac{\partial x}{\partial \upsilon}\right]^2 + \left[\frac{\partial y}{\partial \upsilon}\right]^2 + \left[\frac{\partial z}{\partial \upsilon}\right]^2 \quad \text{(A12)}$$

then the direction-cosines of the normals to the three surfaces which pass through (x,y,z) are as follows:

$$\left[h_1 \frac{\partial x}{\partial \lambda}, \quad h_1 \frac{\partial y}{\partial \lambda}, \quad h_1 \frac{\partial z}{\partial \lambda} \right] \qquad \textbf{(A13a)}$$

$$\left[h_2 \frac{\partial x}{\partial \mu}, \quad h_2 \frac{\partial y}{\partial \mu}, \quad h_2 \frac{\partial z}{\partial \mu} \right] \qquad \textbf{(A13b)}$$

$$\left[h_3 \frac{\partial x}{\partial \upsilon}, \quad h_3 \frac{\partial y}{\partial \upsilon}, \quad h_3 \frac{\partial z}{\partial \upsilon} \right] \qquad \textbf{(A13c)}$$

If λ,μ,υ are functions of x,y,z, the direction-cosines of the three line-elements above also can be expressed in the forms:

$$\left[\frac{1}{h_1}\frac{\partial \lambda}{\partial x}, \quad \frac{1}{h_1}\frac{\partial \lambda}{\partial y}, \quad \frac{1}{h_1}\frac{\partial \lambda}{\partial z} \right] \qquad \textbf{(A14a)}$$

$$\left[\frac{1}{h_2}\frac{\partial \mu}{\partial x}, \quad \frac{1}{h_2}\frac{\partial \mu}{\partial y}, \quad \frac{1}{h_2}\frac{\partial \mu}{\partial z} \right] \qquad \textbf{(A14b)}$$

$$\left[\frac{1}{h_3}\frac{\partial \upsilon}{\partial x}, \quad \frac{1}{h_3}\frac{\partial \upsilon}{\partial y}, \quad \frac{1}{h_3}\frac{\partial \upsilon}{\partial z} \right] \qquad \textbf{(A14c)}$$

Equating the terms in Equation A14 with Equation A13 and substituting with Equations A7–A9 gives the following:

$$\frac{\partial \lambda}{\partial x} = h_1^2 \frac{\partial x}{\partial \lambda} = \frac{1}{2} h_1^2 \frac{x}{a^2 + \lambda} \qquad \textbf{(A15)}$$

$$\frac{\partial \lambda}{\partial y} = h_1^2 \frac{\partial y}{\partial \lambda} = \frac{1}{2} h_1^2 \frac{y}{b^2 + \lambda} \qquad \textbf{(A16)}$$

$$\frac{\partial \lambda}{\partial z} = h_1^2 \frac{\partial z}{\partial \lambda} = \frac{1}{2} h_1^2 \frac{z}{\lambda} \qquad \textbf{(A17)}$$

An expression for h_1^2 can be found using Equations A7–A10

$$h_1^2 = \frac{4(a^2 + \lambda)^2(b^2 + \lambda)^2\lambda^2}{E} \qquad \textbf{(A18)}$$

where

$$E = x^2\lambda^2(b^2 + \lambda)^2 + y^2\lambda^2(a^2 + \lambda)^2 + z^2(a^2 + \lambda)^2(b^2 + \lambda)^2 \qquad \textbf{(10)}$$

The velocity components can be derived as follows:

$$\frac{dx}{dt} = \frac{\partial \phi}{\partial x} \qquad \frac{dy}{dt} = \frac{\partial \phi}{\partial y} \qquad \frac{dz}{dt} = \frac{\partial \phi}{\partial z} \qquad \textbf{(A19)}$$

Using the chain rule:

$$\frac{\partial \phi}{\partial x} = \frac{d\phi}{d\lambda}\frac{\partial \lambda}{\partial x} \qquad \frac{\partial \phi}{\partial y} = \frac{d\phi}{d\lambda}\frac{\partial \lambda}{\partial y} \qquad \frac{\partial \phi}{\partial z} = \frac{d\phi}{d\lambda}\frac{\partial \lambda}{\partial z} \qquad \textbf{(A20)}$$

An expression for $d\phi/d\lambda$ can be obtained by differentiating Equation A1:

$$\frac{d\phi}{d\lambda} = \frac{Q}{4\pi[(a^2 + \lambda)(b^2 + \lambda)\lambda]^2} \qquad \textbf{(A21)}$$

Substitution of Equation A21 and Equations A15–A17 into Equation A20 gives

$$V_x = \frac{dx}{dt} = \frac{\partial \phi}{\partial x} = \frac{Qx(a^2 + \lambda)^{1/2}(b^2 + \lambda)^{3/2}\lambda^{3/2}}{2\pi E} \qquad \textbf{(A22)}$$

$$V_y = \frac{dy}{dt} = \frac{\partial \phi}{\partial y} = \frac{Qy(a^2 + \lambda)^{3/2}(b^2 + \lambda)^{1/2}\lambda^{3/2}}{2\pi E} \qquad \textbf{(A23)}$$

$$V_z = \frac{dz}{dt} = \frac{\partial \phi}{\partial z} = \frac{Qz(a^2 + \lambda)^{3/2}(b^2 + \lambda)^{3/2}\lambda^{1/2}}{2\pi E} \qquad \textbf{(A24)}$$

The velocity also may be obtained by related rate differentiation:

$$\frac{d\phi}{dt} = \frac{\partial \phi}{\partial x}\frac{dx}{dt} + \frac{\partial \phi}{\partial y}\frac{dy}{dt} + \frac{\partial \phi}{\partial z}\frac{dz}{dt} \qquad \textbf{(A25)}$$

where the x, y and z coordinates of a fluid element moving under the influence of the hood are defined as functions of time. Again for potential flows:

$$\frac{\partial \phi}{\partial x} = \frac{dx}{dt} \qquad \frac{\partial \phi}{\partial y} = \frac{dy}{dt} \qquad \frac{\partial \phi}{\partial z} = \frac{dz}{dt} \qquad \textbf{(A19)}$$

Therefore,

$$\frac{d\phi}{dt} = \left[\frac{dx}{dt}\right]^2 + \left[\frac{dy}{dt}\right]^2 + \left[\frac{dz}{dt}\right]^2 = \left[\frac{ds}{dt}\right]^2 \qquad \textbf{(A26)}$$

where ds is the differential element of arc length along the streamline. The velocity of the air under the influence of suction at any point in front of the hood is

$$ds/dt = (d\phi/dt)^{1/2} \qquad \textbf{(A27)}$$

Using the chain rule,

$$\frac{d\phi}{dt} = \frac{d\phi}{d\lambda}\frac{d\lambda}{dt} \qquad \textbf{(A28)}$$

The expression for $d\phi/d\lambda$ is given in Equation A21.

As described in the text, the use of the exact solution in describing actual velocity fields is somewhat limited. Using the assumption that equipotential surfaces are surfaces of constant velocity, $d\lambda/dt$ can be approximated by the following equation:

$$\frac{d\lambda}{dt} = \frac{\frac{dV}{dt}}{\frac{dV}{d\lambda}} \qquad \textbf{(A29)}$$

where V is the volume enclosed by the equipotential surface (an ellipsoid of unequal axes). If

$$V = (4\pi/3)(a^2 + \lambda)^{1/2}(b^2 + \lambda)^{1/2}\lambda^{1/2}$$

then

$$\frac{dV}{d\lambda} = \frac{2\pi}{3}\left[\frac{3\lambda^2 + 2(a^2 + b^2)\lambda + a^2b^2}{[\lambda^3 + (a^2 + b^2)\lambda^2 + a^2b^2\lambda]^{1/2}}\right] \qquad \textbf{(A30)}$$

The change in volume with time is equal to 2Q. The factor of 2 is included to account for the potential surfaces being half ellipsoids. Substitution of the above expressions into Equation A28 gives the following:

$$\frac{d\phi}{dt} = \frac{3\,Q^2}{4\pi^2[3\lambda^2 + 2(a^2 + b^2)\lambda + a^2b^2]} \quad \textbf{(A31)}$$

and

$$\frac{ds}{dt} = \frac{\sqrt{3}Q}{2\pi[3\lambda^2 + 2(a^2 + b^2)\lambda + a^2b^2]^{1/2}} \quad \textbf{(A32)}$$

Equation A32 gives the magnitude of the velocity at any point in space. The direction of the velocity vector can be determined using the exact solution, (Equations A22–A24). Equation A32 is the approximate solution given in the text as Equation 11, and Equations A22–A24 are the exact solutions given in the text as Equations 7–9.

22 June 1987; Revised 23 January 1988